Assessing Effect of Droughts and Heatwaves on Indian Tropical Forests using Time-Series Meteorological and Vegetation Biophysical Parameters

Hitendra Padalia, Lipsa Pradan, Rohan M S
hitendra@iirs.gov.in, pradhanlipsa1996@gmail.com, rohanmscof@gmail.com

Forestry and Ecology Department, Indian Institute of Remote Sensing (IIRS), Dehradun, 248001, India

Keywords: Drought, Heatwaves, SPI, GPP, ET, Tropical Forests

Abstract

Heat waves and droughts are recurring global phenomena that profoundly influence terrestrial ecosystems. This study assessed the impacts of drought and heat waves on the functioning of tropical evergreen (Kerela, South India) and moist deciduous (Barkot, North India) forest sites using meteorological and satellite vegetation products, including the FAPAR, SIF, GPP, and ET during 2007– 2018. The SPI, calculated from ERA5 daily data, was used to identify drought occurrences in space and time, while the Mann–Kendall test detected historical trends. Heat waves were characterized using hourly maximum temperature data from ERA5, following the criteria of IMD. Temporal anomalies were quantified using Z-scores, along with the Mann–Kendall trend test and Theil–Sen's slope analysis. Moist deciduous showed consistent and pronounced declines in productivity and moisture related variables during droughts, particularly during monsoon season, indicating strong sensitivity to water stress. Evergreen forests exhibited more variable responses, with weaker and less consistent drought signals during the pre-monsoon season and mixed responses in vegetation variables even during monsoon drought conditions. Heat wave impacts also varied across forest types. Evergreen forests showed contrasting responses depending on the timing of heatwave events, with early and mid-heatwave phases associated with reductions in productivity, while late heatwave events showed relatively positive or mixed responses among vegetation indicators. In moist deciduous, heatwaves resulted in more consistent negative anomalies in productivity-related variables, although some years exhibited contrasting behaviour in SIF relative to other indicators. The findings underscore the heterogeneous response of forest ecosystems to extreme climatic events.

1. Introduction

The terrestrial ecosystem successfully slows the rate of global warming by absorbing a significant amount of anthropogenic CO2 emissions, yet substantial uncertainty remains regarding how vegetation will react to future climatic and environmental shifts (Quéré et al., 2018). These occurrences typically exert direct effects on carbon cycles by reducing water availability, decreasing vegetation productivity, and controlling soil respiration, while also triggering indirect effects through time-lag responses, concurrent forest fires, and tree mortality (Ciais et al., 2005; Anderegg et al., 2012, 2015; Page et al., 2002). Because of these interrelated, nonlinear effects, even slight changes in the equilibrium of terrestrial ecosystems brought on by climatic extremes result in significant, intricate changes to the carbon, water, and energy cycles (Ciais et al., 2005). The water and carbon cycles are closely interconnected through photosynthesis; during periods of drought and heat waves, rising air temperatures and falling precipitation can lead to cellular damage in plants and a decline in productivity (Wang et al., 2019; Song et al., 2018).

The impact of these extremes has been observed globally, such as the 2015–2016 El Niño event in the Amazon which reduced gross primary production (GPP) and net carbon uptake (Qian et al., 2019; Sun et al., 2015). While GPP initially increases with rising air temperature, it declines beyond a specific optimal temperature due to the impairment of carboxylation and electron transport processes (Fu et al., 2020). These events also disrupt the vegetation canopy, causing leaf withering and senescence, which can be monitored via the leaf area index (LAI). Physiological responses occur on a timescale of minutes to days, whereas canopy structural changes manifest over weeks. This response varies by ecosystem and species; for instance, trees with deeper roots exhibit higher tolerance to soil water stress (Zhang et al., 2016).

During the 2003 European drought, GPP declined by approximately 30% due to soil dryness and water stress, which led to stomatal closure and reduced evapotranspiration (ET) (Ciais et al., 2005). Multiple studies suggest that this decline in GPP is primarily driven by water stress rather than heat stress (Granier et al., 2007; Reichstein et al., 2007). This water deficit also reduces terrestrial ecosystem respiration (TER), but because the decrease in TER does not fully compensate for the GPP loss, it results in a net decrease in net ecosystem exchange (NEE) and an abnormal release of CO_2 to the atmosphere (Ciais et al., 2005). Comparatively, the 2018 European drought caused NEE anomalies that were only 42% to 75% of the magnitude observed in 2003 (Rödenbeck et al., 2020).

In situ measurements from the 2003 drought confirm that when soil moisture drops below a critical threshold, both GPP and ecosystem respiration experience significant reductions (Granier et al., 2007; Vetter et al., 2008). This is often driven by a combination of soil drought and high vapour pressure deficit (VPD) leading to stomatal closure (Sippel et al., 2018). Under acute drought, ET and GPP decline simultaneously and non-linearly with rising VPD (Gao et al., 2017). Assessing drought-induced ET alterations is complicated by the interplay of variables such as surface air temperature, soil moisture, and water storage (Vicente-Serrano et al., 2010; Kim and Rhee, 2016; Keyantash and Dracup, 2004). While precipitation is the primary driver of drought, the combination of precipitation and temperature drives concurrent heatwaves. Ultimately, drought-induced changes are complex processes heavily influenced by the underlying ecosystem and vegetation species (Leifsson et al., 2015).

The present study assesses the impact of meteorological drought and heatwaves on the functioning of tropical broadleaved evergreen and tropical broadleaved moist deciduous forests using optical and thermal indices.

This contribution has been peer-reviewed.
https://doi.org/10.5194/isprs-archives-XLIX-B3-2026-1029-2026

2. Methodology

2.1 Study Area

The study was carried out for two contrasting tropical broadleaved forest functional types in India (Figure 1). Tropical wet evergreen forest, Western Ghats, Kerela: This study site extends from 9°7'15.6" to 9°33'10.8" N and 76°58'44.4" to 77°20'52.8" E, encompassing parts of Kerala's Periyar National Park and Ranni forest division. The area is located on the western slopes of the Western Ghats, which are known for their unusually high biodiversity. The elevation ranges from 50 to 2000m above mean sea level. These locations receive an average annual rainfall 2800 mm, with high precipitation during both the South-west and North-east monsoons, with maximum rainfall in July and minimum rainfall in January. The annual average temperature ranges from 15°C to 37°C. The vegetation of the area is classified as West Coast Tropical Evergreen Forests (Champion and Seth, 1968).

Tropical moist deciduous forest, Barkot, Uttarakhand: Barkot Reserve Forest (30°03'52" to 30°10'43" N and 78°09'49" to 78°17'09" E), in the Indian state of Uttarakhand, is situated in the Himalayan foothills at an elevation of 340 to 560m above mean sea level. The climate in the area is categorized as tropical to subtropical humid, with temperatures ranging from 2°C to approximately 41°C. The average annual rainfall is around 1800 mm. According Champion and Seth, (1968), the region falls under the Sub-Group 3C North Indian Tropical Moist Deciduous Forest. The dominating species is Sal (*Shorea robusta*), which forms almost pure stands. Rohni (*Mallotus philippensis*), Sain (*Terminalia tomentosa)* and Dhauri (*Lagerstroemia parviflora*) are common companion plants.

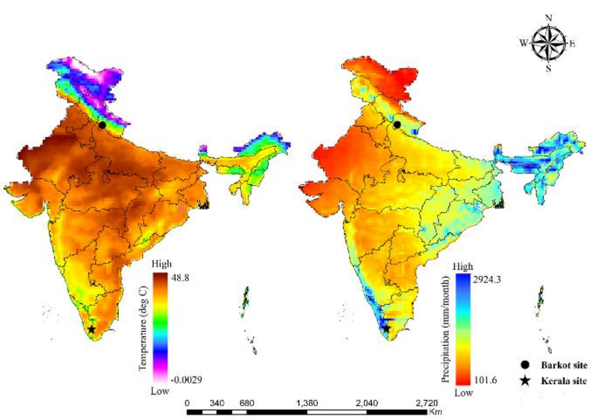

Figure 1. Study sites locations in India along with mean annual temperature and precipitation variability

2.2 Datasets

2.2.1 Climate datasets

ERA-5 data- ERA5 (Fifth Generation of the European Centre for Medium-Range Weather Forecasts Reanalysis) is a worldwide atmospheric reanalysis dataset that covers a wide range of meteorological variables. Temperature and precipitation hourly data was used in the study.

The global climatic zones (IPCC, 2006) are defined by a set of principles based on yearly mean daily temperature, total annual precipitation, total annual potential evapotranspiration (PET), and elevation.

Root zone soil moisture products (GLDAS 2.2) generated by NASA Global Land Data Assimilation System (GLDAS) project was used. It estimates root zone soil moisture at various spatial and temporal scales.

2.2.2 MODIS Vegetation Products

8-day composite products of MODIS satellite products representing Plant Functional Types (MODIS/061/MCD12Q1), Fraction of Photosynthetically Active Radiation (FPAR) (MODIS/061/MOD15A2H), GPP (MODIS/006/MOD17A2H) and ET (MODIS/006/MOD16A2) at a spatial resolution of 500m were used.

2.2.3 Vegetation Indices

Vegetative indices viz., VCI (Vegetation Condition Index), TCI (Temperature Condition Index), and VHI (Vegetation Health Index) were acquired using NOAA STAR's AVHRR and VIIRS blended products.

2.2.4 GOME-2 SIF Product

Monthly GOME-2 ((Global Ozone Monitoring Experiment-2) SIF level 3 product from 2007 to 2018 were used in this study. GOME-2 is an imager with worldwide coverage, a spatial resolution of 40*40km, and a swath of 1920km. The wavelength range 740-780 nm data is given in units of W/m2/sr/m, in NetCDF format. The products are monthly averaged and gridded, with negative values considered as zero.

2.2.5 NOAA STAR - Vegetation Health Products

Blended-VHP is a reprocessed dataset of Vegetation Health derived from GAC data obtained from VIIRS (2013-present) and AVHRR (1981-2012). VCI, TCI, and VHI are global products that provide drought monitoring with a spatial resolution of 4 km and a 7-day composite.

2.3 Pre-processing of datasets

SIF products were converted from .nc format to geotiff format. The negative values were substituted with zeros. FPAR 8-day data from MOD15A2H.061 was multiplied by scale factor 0.01. Cloud masking was applied on 8-day GPP and ET from MODIS/006/MOD17A2H and MODIS/006/MOD16A2 respectively level 3 products. No correction applied to VCI, TCI, VHI, and Root zone soil moisture. Temperature and precipitation data from ERA5 reanalysis data is delivered to the in user accessible format, no formatting was applied. According to the analysis's requirements, the various temporal scales of distinct variables were averaged or summed to obtain weekly, monthly, or yearly data. R and Python were used to manage and analyse all the data in Netcdf format.

2.4 Identification of Drought

Th hydrometeorological index i.e. Standardised Precipitation Index (SPI) was generated using ERA-5 daily data. SPI was used to assess the drought occurrences in terms of space and time. The Mann-Kendall test was used to examine historical changes.

SPI was estimated at 3-month intervals using long-term daily data (2007-2018) using the R package "SPEI"(Beguería et al., 2014). Mckee et al., (1993), designed it to estimate the rainfall

https://doi.org/10.5194/isprs-archives-XLIX-B3-2026-1029-2026

deficit at various time frames. To identify the droughts that occurred during the monsoon season (JJAS), the cumulative SPI-3 values were calculated, and maps were created for the monsoon seasons from 2007 to 2018. Following SPI-3 calculation, raster images were further classified using the SPI classification table, resulting in the identification of drought occurrences in India throughout the pre-monsoon and monsoon seasons. If the SPI values remained negative for a longer period, the area was considered to have been subjected to a prolonged drought, and vice versa.

2.5 Identification of Heatwaves

According to the Indian Meteorological Department (IMD), a heatwave is declared when the maximum temperature reaches at least 40 °C or higher for plains and at least 30 °C or higher for hilly regions, and the maximum temperature deviation is at least 4 °C-6 °C above normal. At the same time, a severe heatwave is proclaimed if the temperature deviates from the maximum by more than 6 degrees Celsius or the actual maximum temperature is 47°C (Pai et al., 2017). This definition, however, may not account for climatological temperature fluctuations across different locations and seasons. Perkins et al., (2012) propose utilising a time-varying percentile-based threshold technique to characterise heatwaves. This method evaluates the local climate and identifies heatwaves by exceeding defined percentiles of temperature thresholds.

So, before calculating heatwaves, India was divided into five climatic zones, namely alpine, temperate, tropical dry, tropical wet, and tropical moist zones, according to the IPCC's 2006 climatic zone classification. Then, for each climatic zone independently, heat waves were recognised using the 90th percentile threshold of maximum temperatures (Tmax) based on a 3-day window (Tmax90) and then combined to create heatwave maps. This analysis excluded the alpine and temperate climate zones. The 3-day moving window centred on each calendar day was used to account for temporal unpredictability while creating a sufficient sample size to obtain a realistic percentile value. A heat wave is declared when the daily maximum temperature exceeds the 90th percentile criteria of maximum temperature (Tmax) for at least three consecutive days (Rohini et al., 2019). In India, heatwave conditions are normally encountered from March to July, however to determine if dry conditions prevailed from February or not, data from February, March, April, May, and June months were evaluated for each year in the heatwave analysis.

2.6 Statistical analysis

2.6.1 Anomaly detection using Z-score

For drought and heatwave periods, anomalies of the climatic and vegetation functioning variables x are given as absolute differences from the relevant long-term average (Equation 1) and as standard scores (z-scores, Equation 2).

$$\Delta x_i = x_i - \mu \quad \text{...(1)}$$

$$z_i = (x_i - \mu)/\sigma \quad \text{...(2)}$$

Where µ and $\boldsymbol{\sigma}$ stand for, respectively, the mean and standard deviation of the x time series. Anomalies at various locations and periods can be compared in terms of how extreme they are by using the z-score, which indicates by how many standard deviations an observation is above or below its expected value.

2.6.2 Mann-Kendall Trend and Theil-Sen's slope analysis

The impacts of drought and heat waves on vegetation functioning were examined using a combination of Mann-Kendall trend and Theil- Sen's slope analysis. The time series variables viz., GPP, ET, fraction of absorbed photosynthetically active radiation (FPAR), solar-induced fluorescence (SIF), temperature, rainfall, root zone soil moisture, VHI, VCI, and TCI, were analysed.

The Mann-Kendall test (M-K test) (Mann,1945; Kendall,1975) is a non-parametric statistical test that is frequently used in climatology and hydrology to determine whether a monotonic trend is present and if so, in what direction. Finding long-term trends or changes in variables over time is one of its main applications. It has advantages because its calculating approach is straight-forward, and samples do not require certain distributions. Consequently, the M-K technique is frequently used to assess shifting trends and determine the importance of trends in time series for factors such as temperature, precipitation, and drought, among others.

When it comes to the M-K test's statistic Z, $Z > 0$ denotes an upward trend and $Z < 0$ denotes a downward trend. The values of $|Za|$ at the significance levels of 0.01, 0.05, and 0.1 are 2.58, 1.96, and 1.65, respectively. If $|Z| > |Za|$ at a particular level of significance, the statistics pass the appropriate significance test. In addition, a simple non-parametric method known as statistics of slope developed by (Sen, 1968) was also applied. For determining the magnitude and direction of trends in time series data, it is a reliable method. The slope or rate of change of a variable over time is quantified using this analysis. The goal of the study was to quantify the magnitude and direction of changes brought about by drought and heat waves on vegetation by applying Sen's slope analysis to the time series data of the chosen variables. The R trend package was utilised to carry out the Sen's slope and Mann-Kendall trend analysis. Pearson correlation analysis was chosen to study the vegetation's adaptations against drought and heat waves. When $p < 0.05$, the correlation is significant, according to a F-test that was conducted. $R > 0$ and $R < 0$ respectively served as indicators of positive and negative correlation.

3. Results and Discussion

3.1 Impact of drought on tropical evergreen forest

The tropical evergreen forests of Kerala (Figure 2 and Figure 3) experienced drought during 2008, 2012, 2015 and 2016, with the drought signal more distinctly expressed during the monsoon season than in the pre-monsoon season. In the pre-monsoon season (Figure 2), the response is generally mixed across years. In 2008, positive anomalies are observed in SIF and root zone soil moisture, while ET, GPP, FPAR, precipitation, and SPI-3 remain near to or below the zero line, indicating the absence of a strong and consistent drought signal. In 2012, a clearer negative pattern emerges, particularly in ET, GPP, FPAR, precipitation, and SPI-3, suggesting drier antecedent conditions prior to the monsoon. In 2015, most variables remain close to normal with only weak deviations, indicating near-normal pre-monsoon conditions. In contrast, 2016 shows relatively stronger negative anomalies, especially in VHI, precipitation, TCI, and SPI-3, along with reduced values in several vegetation-related variables, indicating the persistence of dry conditions even before the onset of the monsoon.

https://doi.org/10.5194/isprs-archives-XLIX-B3-2026-1029-2026 | © Author(s) 2026. CC BY 4.0 License.

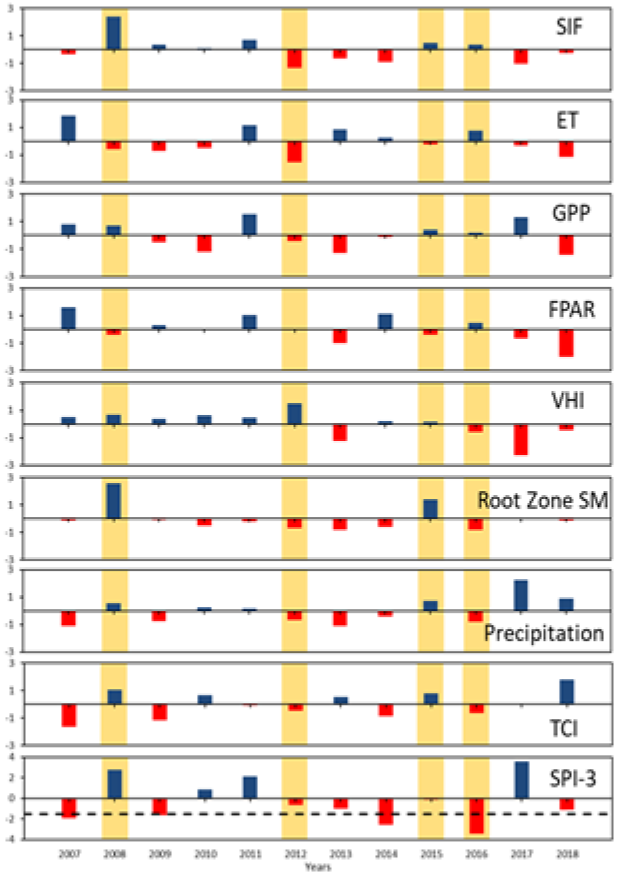

Figure 2. z-score anomaly of variables for drought during pre-monsoon season in Tropical evergreen forest, Kerela

During the monsoon season (Figure 3), the drought signal becomes more coherent and pronounced across variables. In 2008, negative anomalies in precipitation, TCI, and SPI-3 indicate drought conditions; however, vegetation-related variables such as SIF, ET, GPP, FPAR, VHI, and root zone soil moisture exhibit positive anomalies, indicating a contrasting response between hydro-meteorological and vegetation indicators. In 2012, drought conditions are again evident through negative anomalies in precipitation, root zone soil moisture, and SPI-3, while SIF, GPP, and FPAR remain closer to neutral or slightly negative, reflecting a less uniform response. In 2015, despite near-normal pre-monsoon conditions, the monsoon season shows clear drought signals with negative anomalies in precipitation, root zone soil moisture, TCI, and SPI-3, along with a negative VHI, indicating reduced vegetation health. However, GPP, ET, FPAR, and SIF display relatively positive or near-neutral anomalies, suggesting that vegetation activity and productivity were maintained despite reduced water availability. In 2016, drought conditions persist from the pre-monsoon into the monsoon season, with negative anomalies consistently observed in GPP, ET, FPAR, VHI, precipitation, and SPI-3, indicating reduced productivity, lower evapotranspiration, and overall decline in vegetation condition.

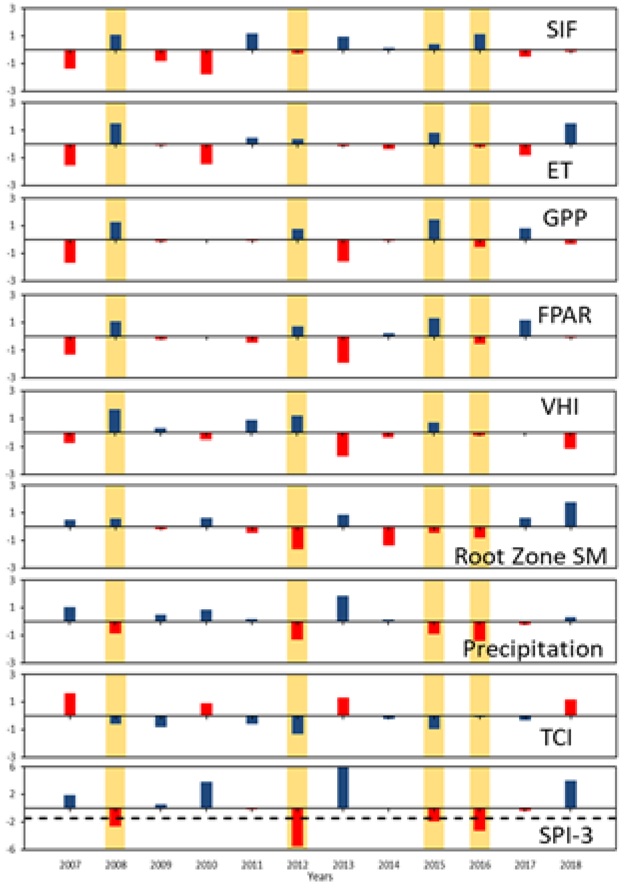

Figure 3. z-score anomaly of variables for drought during monsoon in Tropical evergreen forest, Kerela

Overall the results show a transition from near-normal pre-monsoon conditions to clear drought stress during the monsoon, with reduced vegetation health but positive productivity in most drought years.

3.2 Impact of drought on tropical moist deciduous forest

The tropical moist deciduous forest in Barkot (Figure 4 and Figure 5) experienced drought during 2009, 2012, 2014 and 2015, with the drought signal more consistently expressed during the monsoon season. In the pre-monsoon season (Figure 4), 2009 shows predominantly negative anomalies across GPP, ET, SIF, VHI, root zone soil moisture, precipitation, TCI, and SPI-3, indicating dry antecedent conditions and reduced ecosystem functioning. In 2012, the pre-monsoon season is also characterized by negative anomalies in precipitation, soil moisture, and SPI-3, along with reductions in GPP and FPAR, while ET and SIF appear relatively less negative or closer to neutral. In contrast, 2014 and 2015 show near-normal to slightly positive anomalies in several variables during the pre-monsoon period, particularly in soil moisture, precipitation, and vegetation-related indicators, suggesting the absence of strong pre-monsoon drought conditions in these years.

During the monsoon season (Figure 5), the drought signal becomes more pronounced and consistent across variables. In 2009, strong negative anomalies are observed in GPP, ET, SIF, VHI, root zone soil moisture, precipitation, and SPI-3, indicating a substantial decline in photosynthetic activity, evapotranspiration, and overall vegetation condition under drought stress. In 2012, drought conditions are also evident, with negative anomalies in precipitation, soil moisture, SPI-3, GPP, and FPAR, while ET and SIF show relatively weaker negative responses, suggesting partial maintenance of ecosystem activity. In 2014 and 2015, despite near-normal pre-monsoon conditions, the monsoon season exhibits strong negative anomalies in GPP, ET, SIF, root zone soil moisture, precipitation, and SPI-3, indicating a marked reduction in productivity and water availability. However, FPAR in these years shows comparatively neutral to slightly positive anomalies, indicating that canopy-level light absorption was not reduced to the same extent as other variables.

Overall, the figures indicate that drought in tropical moist deciduous forests leads to a more synchronized decline in ecosystem productivity and water-related variables, particularly during the monsoon period.

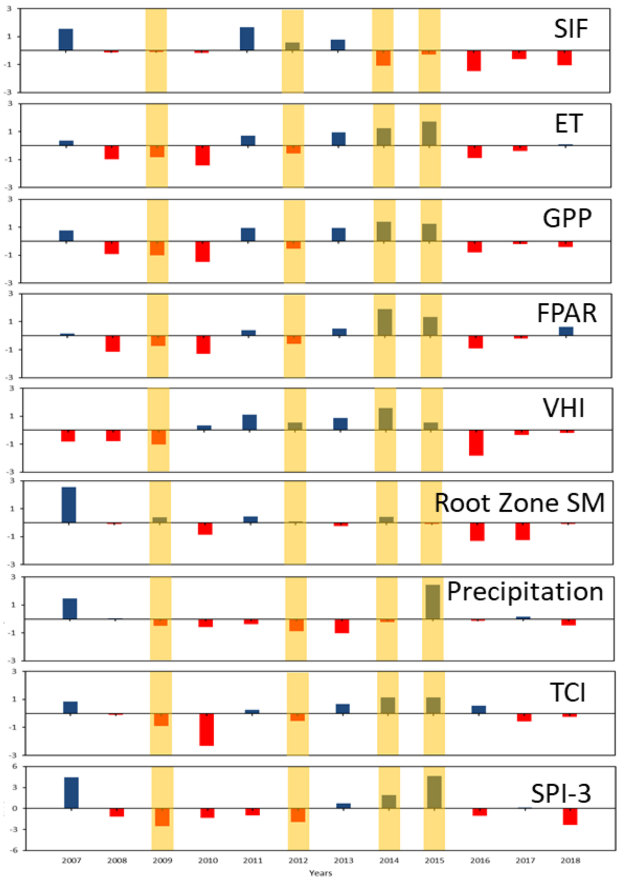

Figure 4. z-score anomaly of variables for drought during pre-monsoon season in Tropical Moist Deciduous Forest, Barkot

3.3 Impact of heatwave on tropical evergreen forest

The tropical evergreen forest of Kerala (Figure 6) experienced distinct heatwave events during 2009, 2010, and 2014, while 2007, 2008, 2011, 2013, 2015, 2017 and 2018 were identified as normal years. The heatwaves occurred during the FMAMJ (February–June) period and were categorized into early (2009), mid (2010), and late (2014) phases based on their timing within the season. In 2009, during the fourth week of February, there was an early heatwave that lasted for a week. An entire week of the second week of March in 2010 saw the mid-heatwave. Lastly, in the final week of March of 2014, a late heatwave lasted for five days. These heatwave years were characterized by relatively higher temperatures compared to normal years, along with reduced precipitation and root zone soil moisture, indicating the presence of heat-induced moisture stress.

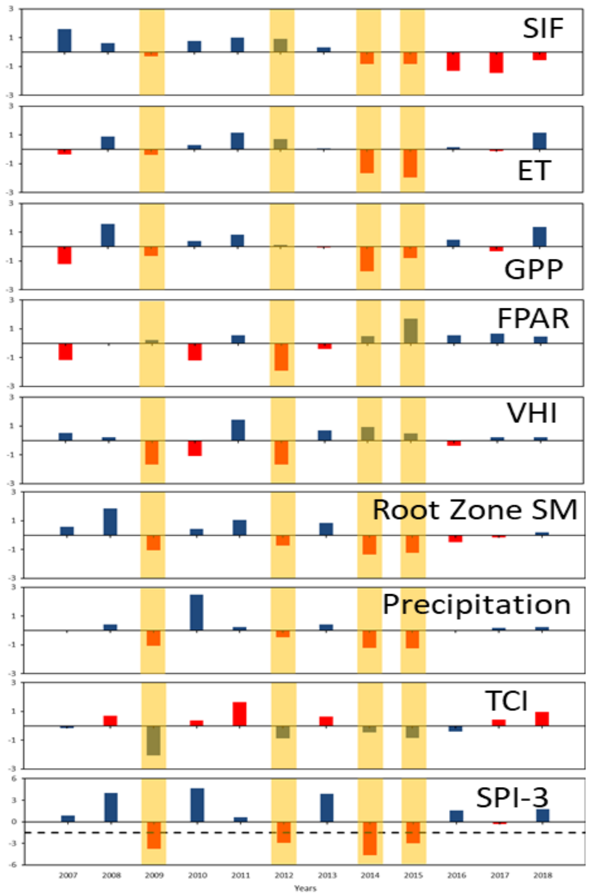

Figure 5. z-score anomaly of variables for drought during monsoon in Tropical Moist Deciduous Forest, Barkot

During the early heatwave in 2009, negative anomalies were observed in GPP and ET, indicating a reduction in productivity and evapotranspiration. In contrast, FPAR and SIF showed positive anomalies, suggesting increased light absorption and enhanced fluorescence response despite reduced water availability. In the mid-heatwave event of 2010, the negative anomaly in GPP became more pronounced, while ET remained near neutral to slightly negative. At the same time, FPAR and SIF continued to show positive anomalies, indicating sustained canopy-level activity despite reduced carbon uptake. In the late heatwave event of 2014, both GPP and ET exhibited positive anomalies, indicating increased productivity and evapotranspiration, while FPAR also remained positive. However, SIF showed a negative anomaly during this period, indicating a contrasting response in photosynthetic efficiency.

Overall, the response of vegetation variables to heatwave events shows clear variability depending on the timing of the heatwave. The early and mid-heatwave phases (2009 and 2010) are characterized by reductions in GPP and ET, along with lower moisture availability, while FPAR and SIF remain positive. In contrast, the late heatwave phase (2014) shows positive anomalies in GPP, ET, and FPAR, but a decline in SIF, indicating a different response pattern. These observations suggest that the impact of heatwaves on tropical evergreen forests varies across the season, with differing responses in productivity, evapotranspiration, and photosynthetic indicators.

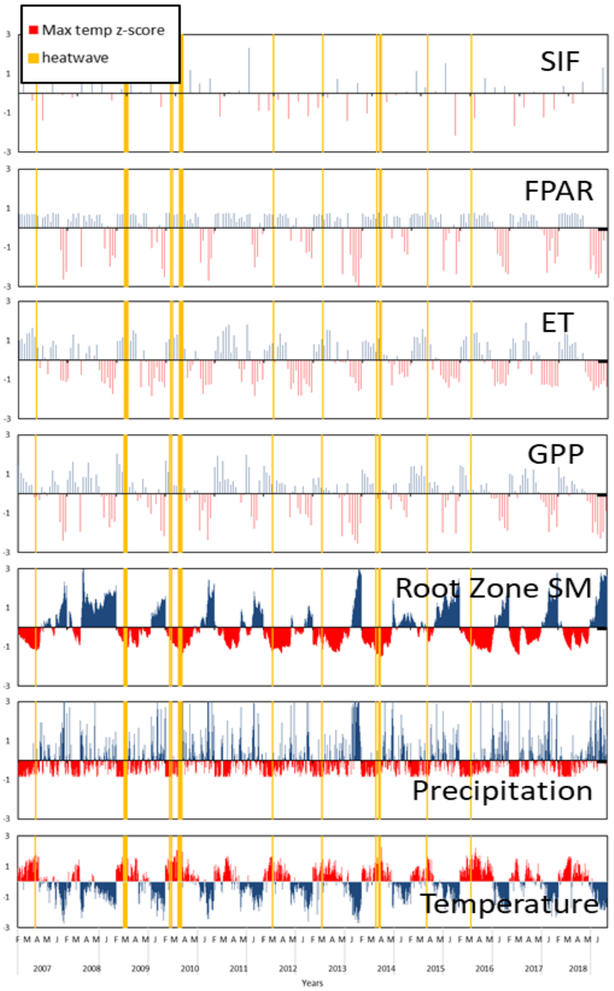

Figure 6. z-score anomaly of variables for heatwave for Tropical evergreen forest, Kerala

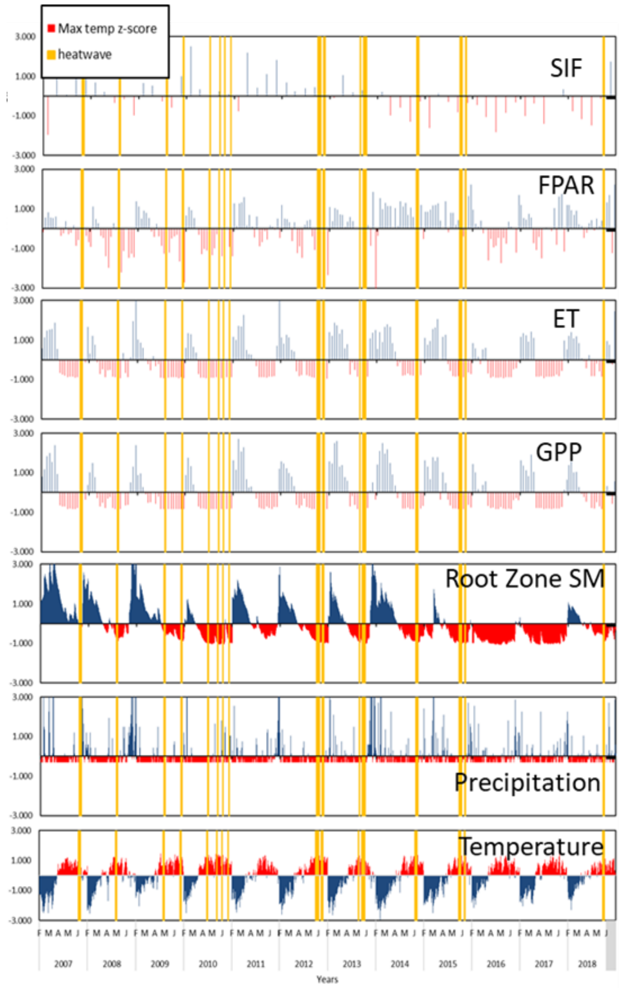

Figure 7. z-score anomaly of variables for heatwave for Tropical moist deciduous forest, Barkot

3.4 Impact of heatwave on tropical moist deciduous forest

The tropical moist deciduous forest of Barkot, Dehradun (Figure 7) experienced heatwave events during 2010, 2012, 2013, and 2015, while 2007, 2008, 2011, 2014, 2016, 2017, and 2018 were identified as normal years. The heatwave years were characterized by higher temperatures during the FMAMJ (February–June) period, along with reduced precipitation and root zone soil moisture, indicating the presence of heat-induced moisture stress. The anomaly patterns in Figures 7 show a consistent response of hydro-meteorological variables, with negative anomalies in precipitation and soil moisture during heatwave years.

In 2010 and 2012, the response of vegetation variables is characterized by predominantly negative anomalies. GPP, ET, and FPAR show clear negative deviations, indicating reduced productivity, lower evapotranspiration, and decreased light absorption under heat stress conditions. At the same time, SIF shows a positive anomaly, indicating a contrasting response compared to other vegetation indicators. This suggests that while overall ecosystem productivity declined, fluorescence response remained elevated during these heatwave events. A similar pattern is observed in 2012, although the magnitude of negative anomalies in GPP, ET, and FPAR appears slightly less pronounced compared to 2010.

In contrast, 2013 shows a different response pattern, where GPP, ET, FPAR, and SIF all exhibit positive anomalies during the heatwave period, indicating an overall enhancement in vegetation activity and ecosystem functioning. In 2015, GPP, ET, and FPAR remain positive, while SIF shows a negative anomaly, indicating a divergence in photosynthetic response compared to structural and productivity-related variables. Overall, the figures indicate that heatwave impacts in tropical moist deciduous forests vary across years, with 2010 and 2012 showing consistent declines in productivity-related variables, while 2013 and 2015 exhibit relatively positive or mixed responses, particularly with contrasting behaviour in SIF.

Tropical deciduous forests face heavy biotic pressures for resource extraction. As this study highlight the vulnerability of these forests of intensifying heat wave and droughts, it vital to reduce biotic degradation and take up restoration activities in these forests to increase their resilience to cope up with extreme climatic events.

4. Conclusions

The study highlights distinct responses of tropical evergreen and moist deciduous forests to drought and heatwave events. Drought impacts were more pronounced during the monsoon season, with consistent declines in moisture-related variables and associated reductions in productivity, especially in moist deciduous forests.

Tropical evergreen forests exhibited relatively mixed and sometimes decoupled responses between vegetation activity and moisture stress. Heatwave impacts varied with timing and forest type, with early and mid-events generally reducing productivity, while some late events showed partial recovery or mixed responses. Overall, moist deciduous forests showed stronger sensitivity, whereas evergreen forests demonstrated comparatively variable and adaptive responses to climatic extremes.

Acknowledgements

Authors are thankful to Director, IIRS and Group Director, AFEG, IIRS for the encouragement and necessary logistic support to conduct the study.

References

Anderegg, W. R. L., Berry, J. A., Smith, D. D., Sperry, J. S., Anderegg, L. D. L., Field, C. B., 2012: The roles of hydraulic and carbon stress in a widespread climate-induced forest die-off. *Proceedings of the National Academy of Sciences of the United States of America*, 109(1), 233–237.

Anderegg, W. R. L., Schwalm, C., Biondi, F., Camarero, J. J., Koch, G., Litvak, M., Ogle, K., Shaw, J. D., Shevliakova, E., Williams, A. P., Wolf, A., Ziaco, E., Pacala, S., 2015: Pervasive drought legacies in forest ecosystems and their implications for carbon cycle models. *Science*, 349(6247), 528–532.

Beguería, S., Vicente-Serrano, S. M., Reig, F., Latorre, B., 2014: Standardized precipitation evapotranspiration index (SPEI) revisited: parameter fitting, evapotranspiration models, tools, datasets and drought monitoring. *International Journal of Climatology*, 34(10), 3001-3023.

Champion, H. G., Seth, S. K., 1968. A Revised Survey of the Forest Types of India.

Ciais, P., Reichstein, M., Viovy, N., Granier, A., Ogée, J., Allard, V., Aubinet, M., Buchmann, N., Bernhofer, C., Carrara, A., Chevallier, F., 2005: Europe-wide reduction in primary productivity caused by the heat and drought in 2003. *Nature*, 437(7058), 529-533.

Fu, Z., Ciais, P., Bastos, A., Stoy, P.C., Yang, H., Green, J.K., Wang, B., Yu, K., Huang, Y., Knohl, A., Šigut, L., 2020: Sensitivity of gross primary productivity to climatic drivers during the summer drought of 2018 in Europe. *Philosophical Transactions of the Royal Society B: Biological Sciences*, 375(1810).

Gao, Y., Markkanen, T., Aurela, M., Mammarella, I., Thum, T., Tsuruta, A., Yang, H., Aalto, T., 2017: Response of water use efficiency to summer drought in a boreal Scots pine forest in Finland. *Biogeosciences*, 14(18), 4409–4422.

Granier, A., Reichstein, M., Bréda, N., Janssens, I. A., Falge, E., Ciais, P., Grünwald, T., Aubinet, M., Berbigier, P., Bernhofer, C., Buchmann, N., 2007: Evidence for soil water control on carbon and water dynamics in European forests during the extremely dry year: 2003. *Agricultural and Forest Meteorology*, 143(1-2), 123-145.

IPCC, 2006. IPCC guidelines for national greenhouse gas inventories.

Kendall, M. G. 1975: *Rank Correlation Methods (4th ed.)*. Charles Griffin, London.

Keyantash, J.A., Dracup, J.A., 2004: An aggregate drought index: Assessing drought severity based on fluctuations in the hydrologic cycle and surface water storage. *Water resources research*, 40(9).

Kim, D., Rhee, J., 2016: A drought index based on actual evapotranspiration from the Bouchet hypothesis. *Geophysical Research Letters*, 43(19), 10,277-10,285.

Leifsson, C., Buras, A., Rammig, A., Naumann, G., Spinoni, J., Vogt, J. V., Barbosa, P., 2015: Assessment of drought damages and their uncertainties in Europe. *Environmental Research Letters*, 10(12), 124013.

Mann, H. B., 1945: Nonparametric tests against trend. *Econometrica: Journal of the Econometric Society*, 245-259.

McKee, T. B., Doesken, N. J., Kleist, J., 1993: The relationship of drought frequency and duration to time scales. *Proceedings of the 8th Conference on Applied Climatology*, 17(22), 179-183.

Page, S.E., Siegert, F., Rieley, J.O., Boehm, H.D.V., Jaya, A., Limin, S., 2002: The amount of carbon released from peat and forest fires in Indonesia during 1997. *Nature*, 420(6911), 61-65.

Pai, D. S., Nair, S. A., Ramanathan, A. N., 2017: *Heat and Cold Waves in India: Processes and Predictability*. Meteorological Monograph No. ESSO/IMD/Met Monograph/01/2017. India Meteorological Department.

Perkins, S. E., Alexander, L. V., 2013: On the measurement of heat waves. *Journal of Climate*, 26(13), 4500-4517.

Qian, X., Qiu, B., Zhang, Y., 2019: Widespread decline in vegetation photosynthesis in Southeast Asia due to the prolonged drought during the 2015/2016 El Niño. *Remote Sensing*, 11(8),910.

Quéré, C., Andrew, R., Friedlingstein, P., Sitch, S., Hauck, J., Pongratz, J., Pickers, P., Ivar Korsbakken, J., Peters, G., Canadell, J., Arneth, A., Arora, V., Barbero, L., Bastos, A., Bopp, L., Ciais, P., Chini, L., Ciais, P., Doney, S., Zheng, B., 2018: Global Carbon Budget 2018. *Earth System Science Data*, 10(4), 2141–2194.

Reichstein, M., Ciais, P., Papale, D., Valentini, R., Running, S., Viovy, N., Zhao, M., 2007: Reduction of ecosystem productivity and respiration during the European summer 2003 climate anomaly: a joint flux tower, remote sensing and modelling analysis. *Global Change Biology*, 13(3), 634-651.

Rödenbeck, C., Zaehle, S., Keeling, R. and Heimann, M., 2020. The European carbon cycle response to heat and drought as seen from atmospheric CO2 data for 1999–2018. *Philosophical Transactions of the Royal Society B: Biological Sciences*, 375(1810).

Rohini, P., Rajeevan, M., Mukhopadhyay, P., 2019: Future projections of heat waves over India from CMIP5 models.

Sen, P. K., 1968: Estimates of the regression coefficient based on Kendall's tau. *Journal of the American Statistical Association*, 63(324), 1379-1389.

Sippel, S., Reichstein, M., Mahecha, M. D., Lange, H., Flach, M., Frank, D., 2018: Drought, heat, and the carbon cycle: a review. *Current Climate Change Reports*, 4(3), 266-277.

Song, L., Guanter, L., Guan, K., You, L., Huete, A., Ju, W., Zhang, Y., 2018: Satellite sun-induced chlorophyll fluorescence detects early response of winter wheat to heat stress in the Indian Indo-Gangetic Plains. *Global Change Biology*, 24(9), 4023-4037.

Sun, Y., Gu, L., Dickinson, R. E., Piao, S., Morales, M. A., Bridgham, S. D., Schwalm, C. R., 2015: Impact of ENSO on continental-scale terrestrial biological productivity. *Nature Communications*, 6(1), 1-11.

Vetter, M., Churkina, G., Jung, M., Reichstein, M., Zaehle, S., Bondeau, A., Heimann, M., 2008: Analyzing the causes and uncertainties of terrestrial biosphere model-simulated carbon flux anomalies during the European summer drought 2003. *Agriculture, Ecosystems & Environment*, 123(1-3), 85-92.

Vicente-Serrano, S. M., Beguería, S., López-Moreno, J. I., 2010: A multiscalar drought index sensitive to global warming: the standardized precipitation evapotranspiration index. *Journal of Climate*, 23(7), 1696-1718.

Wang, J., Xiao, X., Zhang, Y., Chiu, J., Zhou, Y., Qin, Y., Moore, B., 2019: Variations in carbon and water fluxes in a subtropical evergreen coniferous forest of southern China. *Agricultural and Forest Meteorology*, 264, 47-63.

Zhang, Y., Xiao, X., Guanter, L., Zhou, S., Ciais, P., Joiner, J., Wu, X., 2016: Precipitation and air temperature drive terrestrial vegetation phenology and carbon dynamics across the Conterminous United States. *Agricultural and Forest Meteorology*, 221, 39-56.

This contribution has been peer-reviewed.
https://doi.org/10.5194/isprs-archives-XLIX-B3-2026-1029-2026